Entanglement Locking in the Unique Elasticity of Polydimethylsiloxane Rubbers

Vincenzo Villani* and Vito Lavallata

Università degli Studi della Basilicata, Dipartimento di Scienze, Campus Macchia Romana, 85100 Potenza, Italy

vincenzo.villani@unibas.it

Abstract

The viscoelasticity behavior of the Polydimethylsiloxane (PDMS) rubber blends of high molecular weight polymer modified by low molecular weight agent has been studied in compression mode by the stress-strain curves, the creep and step-strain, and dynamic-mechanical experiments.

Elastic behaviors were strongly dependent on the composition: the mechanical experiments in the field of small strain have shown a maximum of elasticity at 4% of the short chain blending agent. On the contrary, in the field of large strain, the maximum elasticity of the blends corresponds to the concentration of 12%. The strain spectra highlight the dynamics of active chains at high frequencies and of dangling ends in the low frequencies field. At low deformation, the blending agent enhances the elastic properties by increasing the density of the active chains in the rubber network, in agreement with the classical theories of elasticity. At high deformation, in analogy with our rheological studies on similar liquid blends, the Entanglement Locking model has been proposed: the short chains of the blending agent would be adsorbed on entanglement sites of long dangling chains, giving effective crosslinks by high entropy dynamics. In this way, the long-term entanglement locking enhances the density of active chains and elastic behavior.

At high deformation, the Entanglement Locking model enriches the rubber elasticity theories according to the tube network model and Mooney-Rivlin equation. The models and the chance of improving the rubber viscoelasticity are valuable attempts for polymer physics and technology and might be considered as a novelty.

Keywords. Polymer viscoelasticity; rubber blends; polydimethylsiloxane; rubber elasticity theory; dynamic-mechanical analysis.

Introduction

Tube models[1,2] and nonequilibrium molecular dynamics simulations[3] are the current theories of polymer melts viscoelasticity. For long macromolecular chains, the model of isolated random-coils loses its validity due to the entanglement network where the probe chain diffuses in the constrained tube region determined by the self-consistent field of the neighboring chains[4]. In the tube model, the molecular weight M_e through successive entanglements forms coils-blobs with mean-squared end-to-end distance R_e^2 which define the transverse dimension (diameter) of the tube[5,6]. The reptation motions contribute to the longitudinal diffusion of the polymer chain, while only transversal fluctuations are possible. The relaxation of the whole chain is described by the disentanglement time τ_d and the relaxation within the tube by the Rouse time τ_R. Starting from the basic models of Doi-Edwards[5], numerous developments have been made as in Slip-Spring[2] and Dynamic Tube Dilation model of Marrucci[7], in which the disentanglement time $\tau_d^* < \tau_d$ is calculated taking into account a reduced transversal diffusion based on the Marrucci and Graessley constant $\tau_d/\tau_d^* = 2.5$ [8]. Some of our recent articles related to this work are placed in this theoretical framework[9,10]. In our previous article[9], it was demonstrated that the polymer melts of high molecular weight PDMS lightly crosslinked (to weight concentrations of crosslinker $<10^{-3}$) exhibit an anomalous reduction of zero-shear rate viscosity η_0 and a drop of rheological properties. This was interpreted by means of the Nanointerface Slipping model, which proposes the formation of isolated crosslinked nanodomains with an entanglement free interface due to too short dangling chains; in this way, an unentangled interface volume V_{free} with only viscous effects (slip-condition) is realized. We conjectured an Einstein-Batchelor modified equation[9,11] in order to take into account the decrease in zero-shear rate viscosity η_0^* for the nano-suspensions.

In the following article[10], the authors demonstrated that a homologous liquid blend based on short and long PDMS chains behaves as if long chains moved within rigid tubes in which the entanglement sites were stabilized by the adsorption of the short chains on entanglement site (Entanglement Locking model). In contrast, the pure component based on long PDMS chains follows the expected tube dilation model. In the present work the entanglement locking model for polymer melt will be extended to the rubber network.

The rubber elasticity theory was developed starting from the phantom-chain model of the pioneering works of James and Guth[12,13], to the Flory random-coil model[14,15] in which the crosslinked active chains are considered isolated. In the Allegra and Ronca[16] and Flory[17] models, the phantom chains network presents the crosslink bound by a harmonic potential in order to take

into account the entanglement constraints on the active chains. Therefore, Edwards[18] applied the ideas of the tube model to the rubber network: the crosslinked chains fluctuate in a constrained region by the hindrance of the neighboring chains; then, Marrucci[19] considers the active chains bound in a tube network with an additional harmonic potential with respect to transverse displacements from the longitudinal axis of the tube.

From the experimental point of view, random crosslinking produces a wide distribution of chain lengths of the network, difficult to take into account by the theoretical point of view[20] and a theory of real rubber taking into account the network defects is today a hot topic. Monti, Vega et al. (2017) discuss the contribution of trapped-entanglements in the elasticity of polymer networks by means of NMR experiments. They conclude that short chains do not give rise to trapped entanglements. The contribution of trapped entanglements may be equal to the contribution coming from elastically active chains and is independent of crosslinker functionality[21]. Cohen et al. (2010) studied end-linked PDMS: the contribution of the trapped entanglement becomes negligible[22]. Cohen et al. (2006) prepared an interpenetrating polymer network of long or short PDMS chains. They observed an elastic behavior analogous to an unimodal rubber network[23]. In this theoretical framework, the present work is performed.

From an experimental point of view, the PDMS rubbers have been widely studied[24-27], nevertheless a knowledge gap remains in the development, characterization and modeling of rubber blends[20,28,29] which are considered in this study.

In the Flory model[30,31], the affine deformation of the active chains is assumed and a rubber network in which the mean squared distance between adjacent crosslinks is given by the average squared end-to-end distance of the prepolymer. The entropy of the random network is independent of the length of the crosslinked chains and depends only on the density of active chains $\nu = \rho / M_x$, where ρ is the mass density and M_x the crosslinked molecular weight. The stress-strain equation predicted under the affine deformation hypothesis and for engineering stress, reads as:

$$\sigma = \nu k T \lambda^2 \tag{1}$$

that under the incompressibility condition gives:

$$\sigma = \nu k T \left(\lambda - \frac{1}{\lambda^2} \right) \tag{2}$$

In the James and Guth theory (phantom network), the variation of entropy is associated with fluctuations of junctions. In the stress-strain equation, a modulus that takes into account the density of the chains and the functionality f of the crosslinks results:

$$\sigma = \left(1 - \frac{2}{f} \right) \nu k T \left(\lambda - \frac{1}{\lambda^2} \right) \tag{3}$$

Taking into account that the density of active chains is given by $\nu = \mu f/2$ ($f \geq 3$), where μ is the density of crosslink, we get:

$$\sigma = (\nu - \mu)kT\lambda^2 \tag{4}$$

For a sufficiently high functionality, the two models coincide. In our cases, for the crosslinker it is estimated up to seven Si–H active sites[32].

In general, for values of $\lambda < 0.7$ the compression stress-strain curve deviates from the theoretical one (Mooney-Rivlin effect)[33]. There is today a substantial agreement in identifying the causes of this effect in optimizing van der Waals interactions through chains under load[16,34]. The ideal rubber equations are extended by that of Mooney-Rivlin (derived from continuum mechanics approaches) which takes into account the strain-hardening observed in the compression curve, according to the equation:

$$\sigma = 2\left(C_1 + \frac{C_2}{\lambda}\right)\left(\lambda - \frac{1}{\lambda^2}\right) \tag{5}$$

where $2C_1 = \nu kT$ (Flory modulus) and $2C_2/\lambda$ is the correction factor of the ideal rubber network equations.

A model of rubber deformation that takes into account the role of entanglement is developed by Marrucci in the assumption that the tube cross section deforms affinely[19]. An elastic modulus greater than that of Flory $G = \nu kT$ results:

$$G = A\nu kT = \left(\frac{2}{3} + \frac{r}{3}\right)\frac{l_0}{a_0}\nu kT \tag{6}$$

where A is the amplifying factor, a_0 the tube radius of uncrosslinked polymer, a_r the tube radius of undeformed network ($a_r \geq a_0$), $r = a_0^2/a_r^2$ and l_0 the contour length of the tubes. Then, the amplifying factor A of shear modulus is closely related to the correction factor of Mooney-Rivlin equation:

$$A = \frac{2C_2}{\lambda \nu kT} + 1 \tag{7}$$

Rubinstein and Panyukov (2002) reviewed the elasticity theories and proposed the slip-tube model. They take into account the trapped entanglements (slip-links) between the network strands. In this way, network chains are allowed to fluctuate and redistribute their length along the contour length of their confining tubes. Then, the rubber network modulus is described by two moduli, G_c and G_e, that take into account the density of crosslinks (according to ideal model) and trapped entanglements of chains, respectively[35].

In the present work, due to the high molecular weights of the PDMS, we will have both crosslinked and entanglement networks, for which we will refer to a rubber tube network model in which there

will be active (crosslinked), inactive chains (dangling, loops and free chains) and entanglement network. In particular, we will investigate the role of short chains in stabilizing the entanglement network as in the previous rheology study on uncrosslinked prepolymers, the Entanglement Locking model [11].

Experimental Section

The molecular structure of PDMS prepolymers (base and curing agent) used in this work is shown in **Fig. 1**.

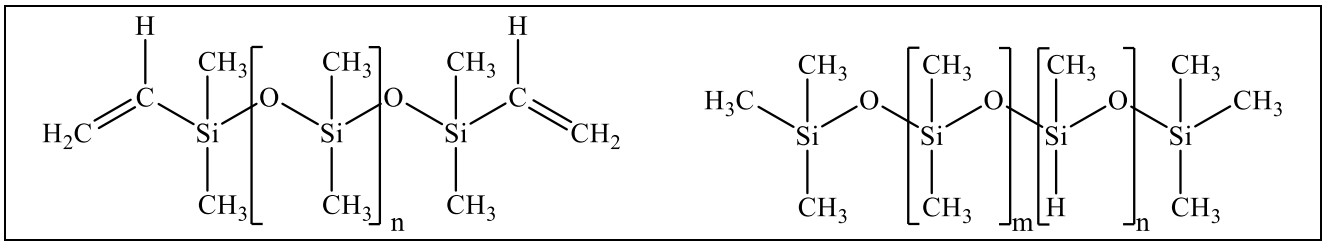

Figure 1. Molecular structures of the vinyl-terminated silicone prepolymer (difunctional α,ω-divinylpoly-(dimethylsiloxane), on the left) and hydride-substituted polysiloxane curing agent (trimethylsilyl terminated poly(dimethylsiloxane-*co*-methylhydrosiloxane), on the right).

The end-linking polymerization, catalyzed by a Pt complex included in the PDMS base, is shown in **Fig. 2**. The vinyl group at prepolymer ends reacts with the methyl-hydrogen-siloxane monomer in the curing agent: the reaction gives at the beginning a polymer grafted, then branched structures and finally, the crosslinked network (**Fig. 2**).

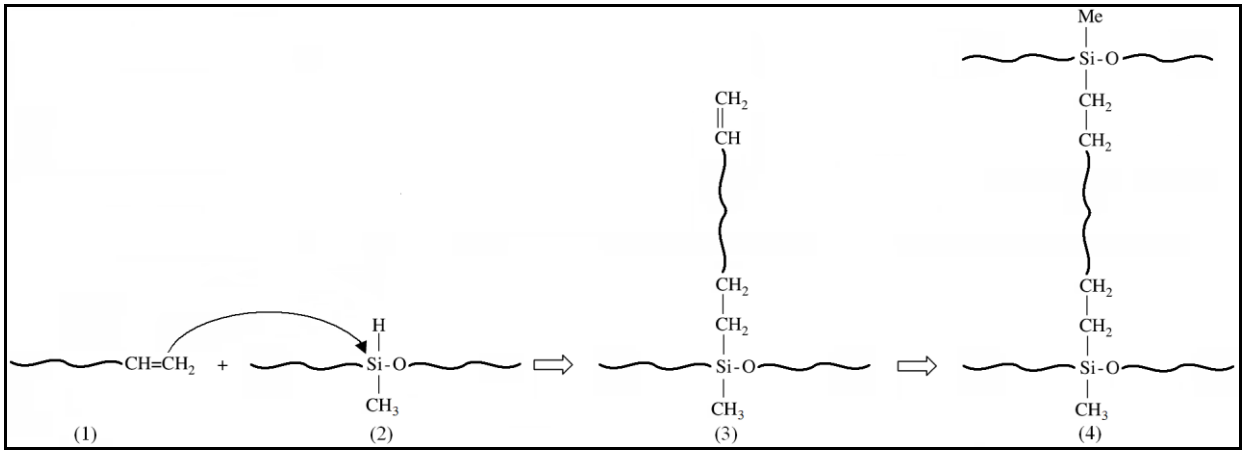

Figure 2. The vinyl-terminated chain of liquid silicone base (1) reacts with the monomethyl siloxane chain of end-linker (2) to give grafted and branched prepolymer chains (3) and finally the rubber network (4).

Liquid silicone rubbers at Low- (L) and Medium-viscosity (M), as defined in the previous papers[9,11], have been considered; Low/Medium homologous rubber blends (L/M) at different L/M ratio have been prepared and cured by means of the medium component crosslinker at 30 °C for at least 3 days in a molding scaffold.

Sylgard® liquid silicone rubbers (Dow Corning) were used. The low-viscous liquid elastomer LE-(L) shows a zero-shear viscosity η_0 = 4.5 P; the medium LE-(M) η_0 = 51 P. In the previous paper[9], we estimated number average molecular weights of M_n(LE-(L))=15,300 unified atomic mass unit and M_n(LE-(M))=43,100. Then, for low LE-(L) $M_n<M_c$ (M_c = 21,000 – 33,000 is the critical molecular weight for the PDMS entangled chain), so LE-(L) is an unentangled liquid prepolymer with n = 113 and the end-to-end distance D_{ee} = 12.2 nm; conversely, LE-(M) is in entangled state with n = 309 and D_{ee} = 20.3 nm[11].

For the PDMS, the entanglement molecular weight M_e is related to M_c as $M_c = 2.4M_e$ [36]. Then, according to the freely-jointed model, the end-to-end distance of the blob is D_{ee} = 13.5 nm, similar to the value of the short chain random coil[11].

The Low-in-Medium rubber blends (L/M20) at 20% of curing agent were prepared at weight percent ratios $p_{L/M} = \frac{LE-(L)}{LE-(M)}100 = 1.9, 4.2, 6.2, 8.2, 12.0\%$ of LE-(L) respect to LE-(M). The samples are summarized in **Table I**.

Therefore, the L/M10 at 10% of curing was prepared at only $p_{L/M}$ = 2.1%: at this content of curing agent, a sticky rubber is obtained, and then this formulation has no longer been thoroughly investigated.

The medium pure components at 10% (M10) and 20% (M20) of curing agent were considered as reference rubbers.

Label	L2/M10	L2/M20	L4/M20	L6/M20	L8/M20	L12/M20
$p_{L/M}$ wt %	2.1	1.9	4.2	6.2	8.2	12.0

Table I. The rubber blends samples at different concentration $p_{L/M}$ of blending agent. In L*x*/M*y*, *x* stands for weight percent ratio $p_{L/M}$ of the blending agent in the rubber, and *y* is the weight percent ratio of curing agent in the rubber.

The Dynamic-Mechanical Analyzer Q800 (TA Instruments) in compression configuration (rubber dishes of 12.67 mm diameter, obtained by means of TA utility, between plates of 15 mm) has been

used. The isothermal experiments at 30 °C were performed.

Pure components and their blends have been characterized in monotonic and oscillating regime. Accurate stress-strain curves at $5 \cdot 10^{-4}$ min^{-1} strain rate, up to the maximum instrumental static force of 18 N, have been performed. By linear fitting of stress-strain curves, the modulus is estimated at low (close to zero strain) and large deformations.

We investigated the compliance $J(t)$ by creep experiments using 30 kPa constant stress and $E(t)$ by stress-relaxation experiments applying 1% constant strain. The strain spectra from 200 to 1 Hz at 0.05% amplitude have been carried out.

Results and Models

In **Fig. 3** the stress-strain experiments in compression mode are reported. The L/M blends varying the low component from 2 to 12% with the curing agent concentrations considered at 10 or 20%. In order to evaluate the elasticity of materials, in **Fig. 6** the Young modulus as a function of blending component concentration is reported. The values are determined at the origin (close to 0% strain) and at ultimate deformation, from curves of Fig. 3, by means of the linear fitting of one hundred points. In **Fig. 7** the stress at the strain value ε = 0.75% (small deformation) and the strain at the stress value $\sigma = 3.6 \cdot 10^{-2}$ MPa (large deformation) from Fig. 6 are plotted in function of the low component concentration.

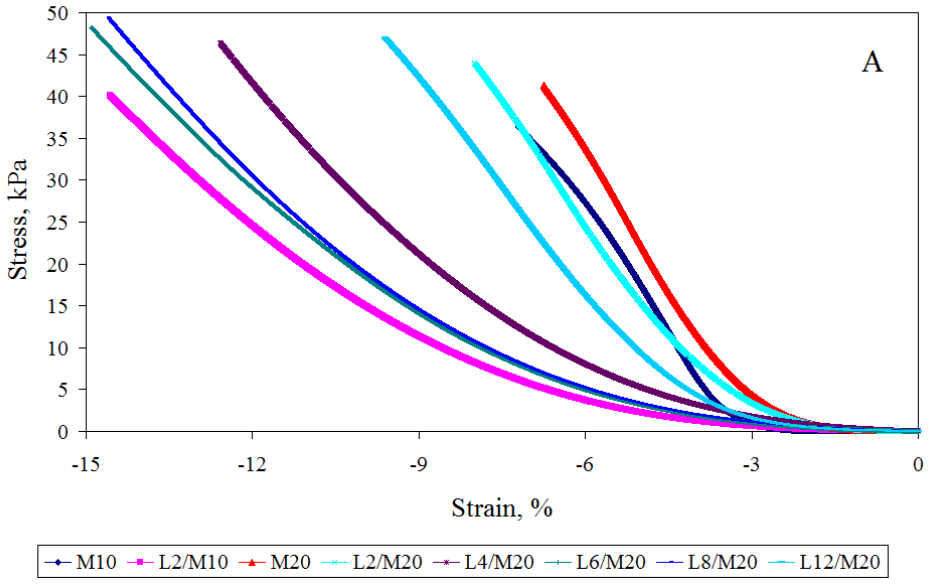

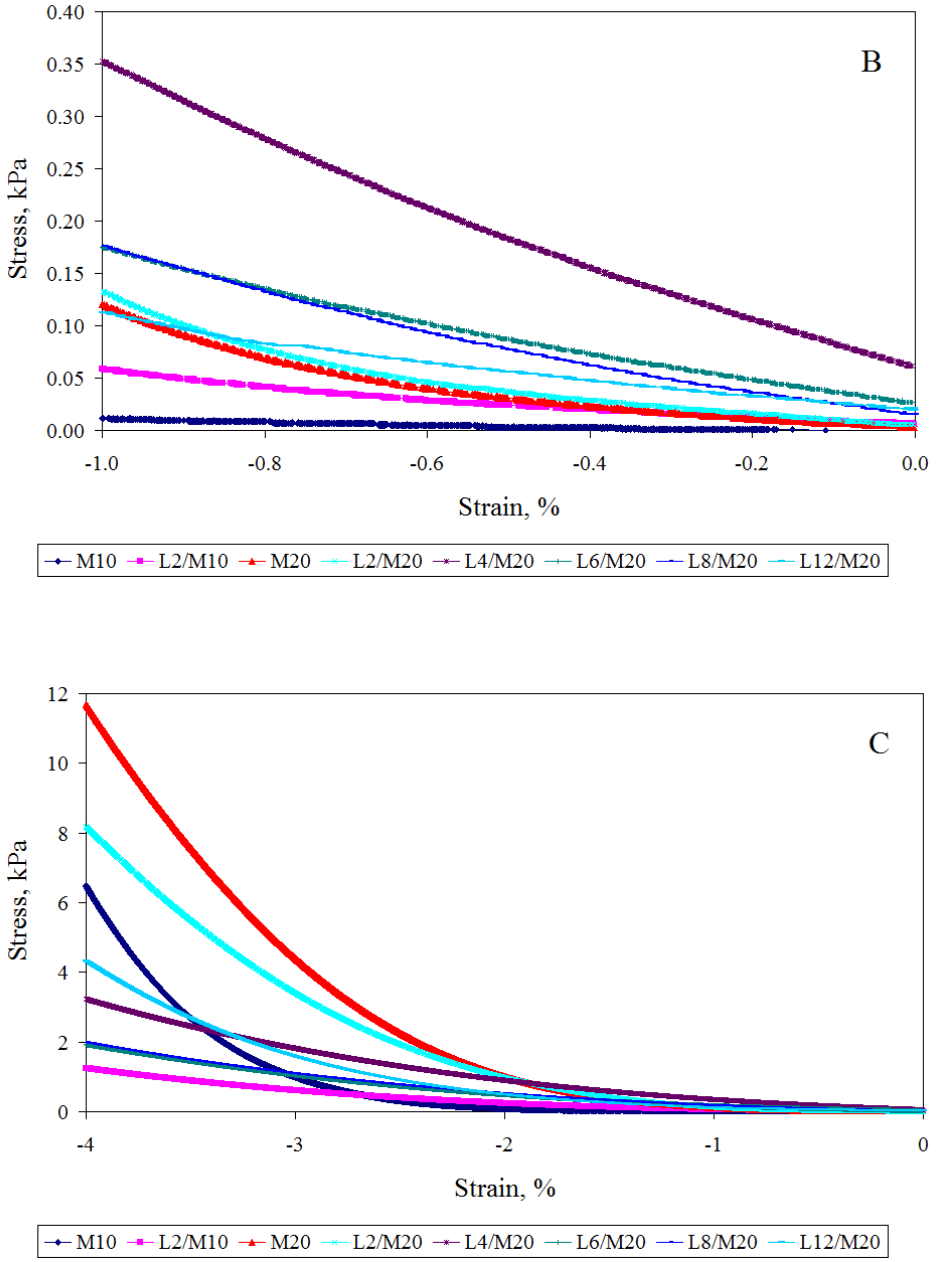

Figure 3. Stress-strain curves in compression mode for L/M rubber blends varying the concentration of low molecular weight blending and curing agents. In (A) is shown the plot up to the maximum instrumental force value of 18 N. In (B) the zooming of (A) up to 1% and in (C) up to 4% of strain.

From the analysis of Figs. 3, 6 and 7, it is evident that the mechanical performance of the rubbers as the blending varies depends on small or large deformations. In fact, at low deformations, the 4% blend is the stiffest, even greater than the medium component. The curve of the elastic moduli (Fig. 6) at low deformations shows an increase up to the maximum at 4% and the subsequent decrease. This behavior is confirmed by the corresponding stress curves for $\varepsilon = 0.75\%$ (at low strain) in Fig. 7 which clearly shows the maximum trend described.

The trend of the high deformation moduli shown in Fig. 6 shows a decrease in the values with respect to the pure component, with a minimum at about 6% of the low component and a subsequent increase up to the composition of 12%. This minimum trend is confirmed by the deformation curves for $\sigma = 3.6 \cdot 10^{-2}$ MPa (at high stress) (Fig. 7).

We analyze the possible molecular picture to take into account the behavior at small or large strains varying the blending component. In agreement with the theories of the ideal rubber, the entropic elasticity is proportional to the temperature and the density of active chains: in this way, the network of low or high components plays a different role.

For the rubber network of the pure component, as the crosslinker concentration increases (from 10 to 20%), a corresponding variation in the elastic modulus is observed. For a perfect network without dangling chains (at stoichiometric concentration of 10% crosslinker), in agreement with the ideal elasticity theories, it is necessary to admit that with increasing crosslink density μ there is a corresponding decrease in functionality f to give the density of active chains $\nu = \mu f / 2$.

On the contrary, for a real network, an increase of μ would have a decrease of the concentration of defects (dangling chains) and a corresponding increase in the density of active chains.

The rubber at 20% crosslinker (at excess concentration of curing agent) would be at low density of dangling chains (Scheme IA). At low blending concentration, the short chains are likely to saturate the available crosslinker –Si–H sites. The achievement of the maximum active chain density and functionality of the crosslinks would account for the maximum elasticity at 4% of the blending component at small strain (Scheme IB).

As the concentration of short chains increases, the long and short chains compete in the binding to the crosslinker, causing an increase in the concentration of dangling chains with the consequent decrease in the density of active chains that would determine the subsequent softness observed at low deformation for concentrations higher than 4% (Scheme IC).

At high deformation, the rigidity reaches the minimum at 6% of the low component. This, according to the theory of elasticity of real rubber, confirms the role of inactive dangling chains at high deformations. Nevertheless, the increase in elasticity for $p_{L/M} > 6\%$ up to the maximum for $p_{L/M} = 12\%$ is unexpected. This effect cannot be due to trapped entanglements, whose density decreases as the concentration of short chains increases. On the contrary, this could be the case with the Entanglement Locking model (Scheme ID).

As discussed in the previous work[11], the entanglement locking is a complex dynamical effect: the short chains cannot give entanglement, but because of their nanometric size, analogous to the blobs of the tube chains, they interact with the entanglement of the long chains by a many-body dynamics that stabilizes entanglements, increasing the lifetime and the entropy of the network.

The proposed conceptual model is based on the increase of the rubber elasticity at large strain and high blending concentration: the locking would behave such as effective junctions, increasing the active chain density and therefore explains the solid-state viscoelastic behavior of elastomeric materials.

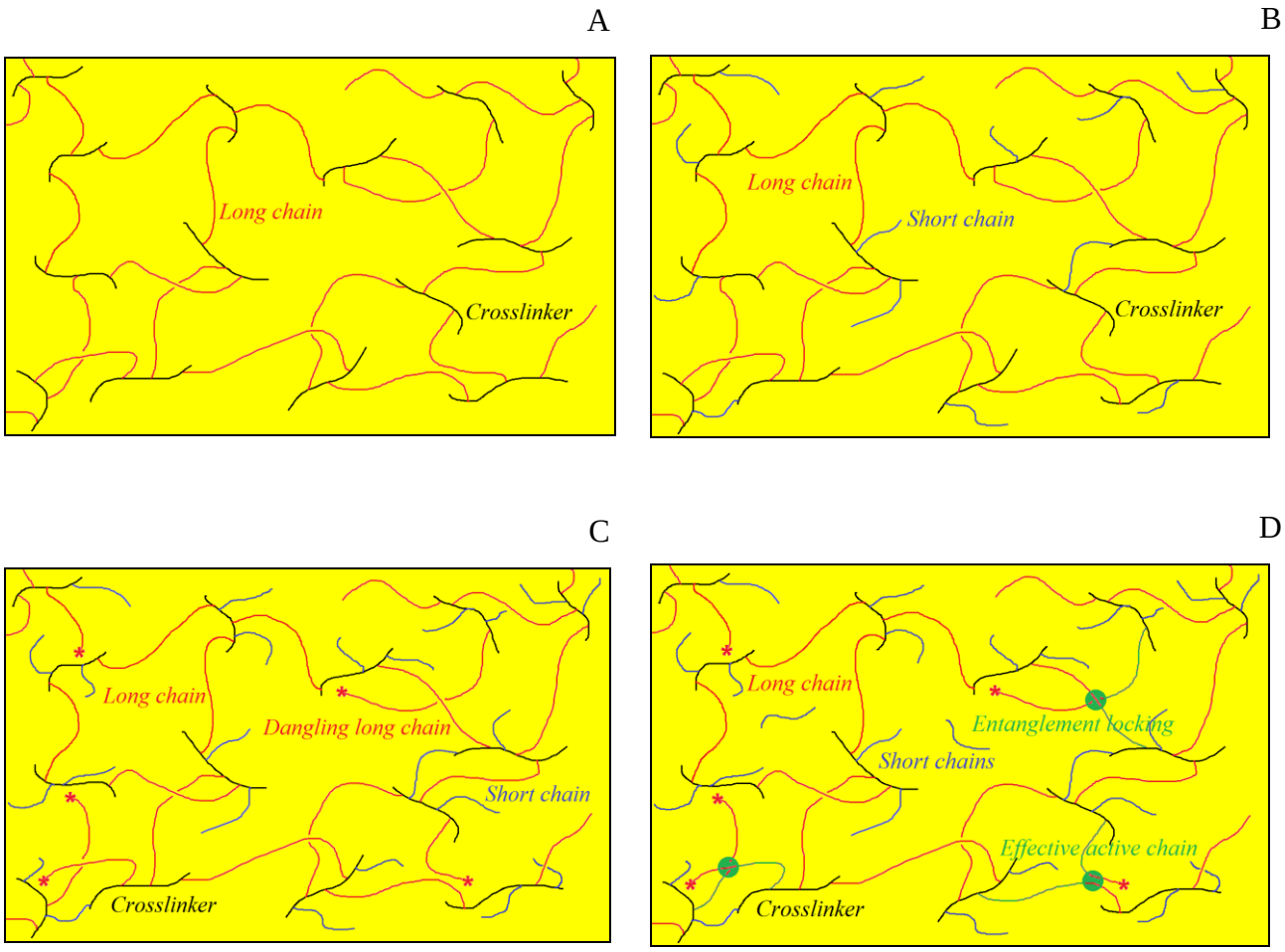

Scheme I. The Entanglement Locking model. The picture highlights the structural changes to the increase in the concentration of the short chain blending agent (in blue) in the rubber blend: in (A) we have the reference rubber network of long chains (in red) and crosslinker (in black); in (B) the short chains are grafted onto the crosslinker; in (C) the short and long chains compete in the saturation of the active sites on the crosslinker, generating long dangling chains (marked by a red star); in (D) at high concentration (greater than 12%wt), the short chains give rise to the Entanglement Locking of the dangling ends (marked by a green circle) giving to effective elastically active strands (in green line).

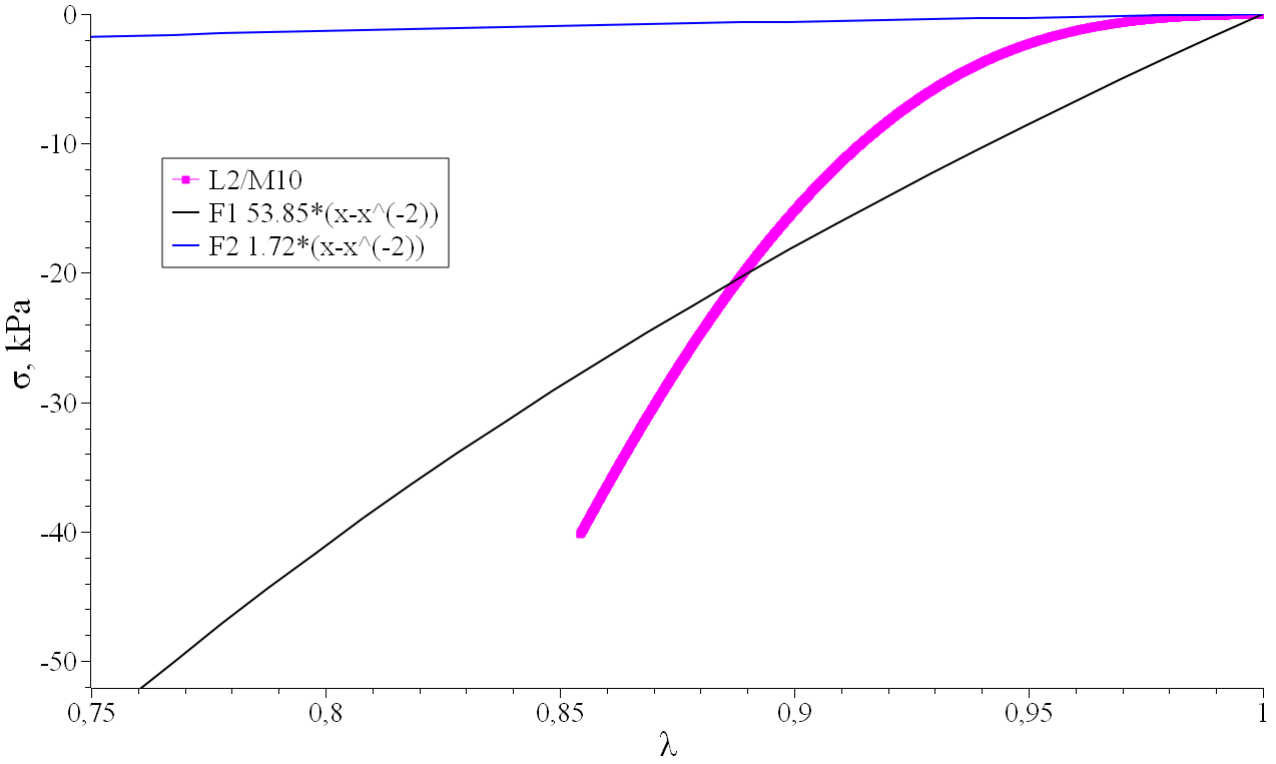

Figure 4. Fitting of the stress-strain curve for the sample L2/M10 by ideal elasticity equations (2-4). The fit curve F1 (in black) is computed on the whole experimental field; the fit curve F2 (in blue) refers to the strain range from 1 to 0.99.

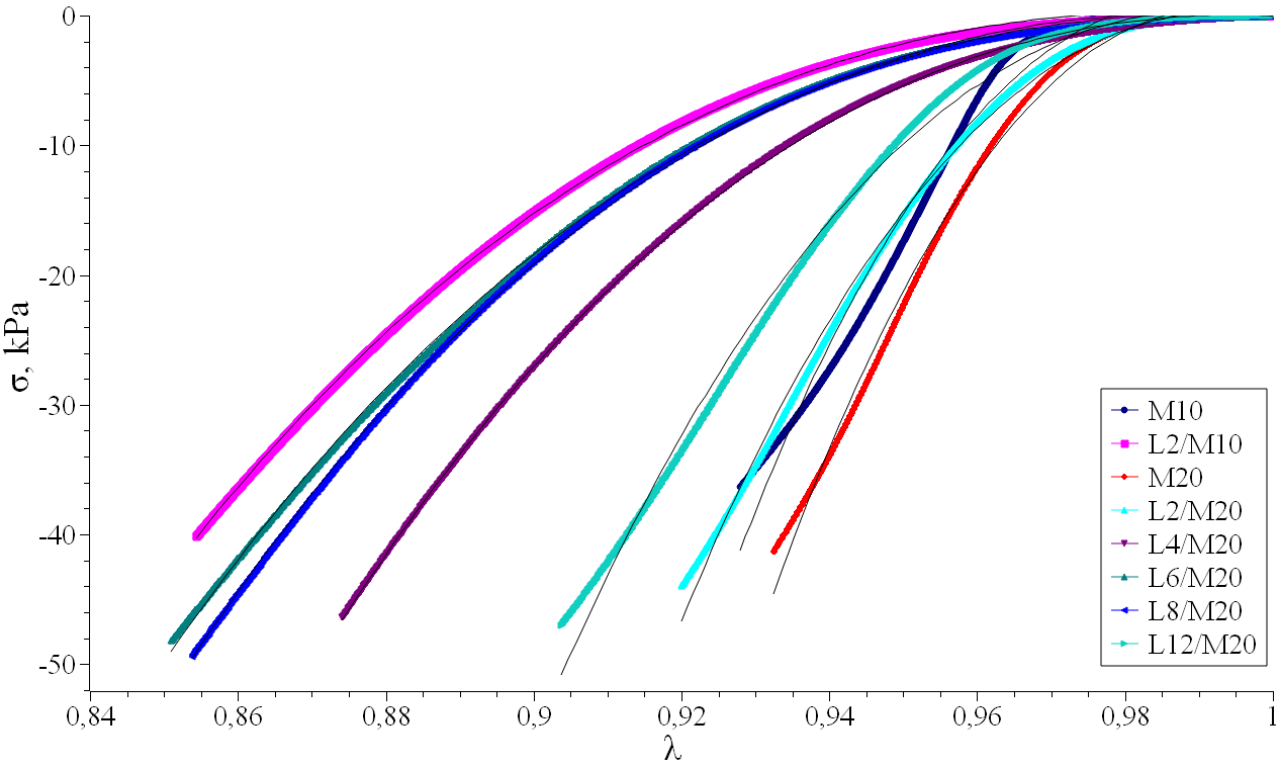

Figure 5. The Mooney-Rivlin fitting of stress-strain compression curves for pure rubbers and blends are reported. The matching is discussed in the text.

In **Fig. 4**, the fitting of the stress-strain for the rubber blend L2/M10 by means of the ideal rubber elasticity equations (2-4) is performed. A badness of fit on the whole experimental field is obtained (R^2 = 0.800), conversely a goodness of fit is obtained in the strain range up to λ = 0.99 (R^2 > 0.968). Similar behavior has occurred in all other cases. To improve the agreement with the theoretical models, the hyperelastic Mooney-Rivlin model will be considered.

In **Fig. 5**, the fitting of the stress-stretching ratio curves $\sigma = f(\lambda)$ for pure rubbers and blends is performed by means of the Mooney-Rivlin equation (7), which takes into account deviations from the ideal rubber theories of equations (3), (5) e (6). The coefficient of determination $R^2 \geq 0.996$ in all cases (except for M10) shows an excellent matching between the experimental data and the theoretical curve. The optimized C_1 and C_2 parameters are summarized in **Table II**.

	L2/M10	M20	L2/M20	L4/M20	L6/M20	L8/M20	L12/M20
C_1	280.780	1 807.153	1 219.459	403.880	297.242	325.797	905.779
C_2	273.254	1 780.634	1 203.972	399.899	292.314	319.005	890.284

Table II. Mooney-Rivlin parameters of the stress-strain compression curves for pure and blend rubbers. C_1 and C_2 values are reported in kPa.

The stress-stretching ratio curve for pure rubber M10 has an R^2 = 0.981 due to the inflection point that requires a Mooney-Rivlin equation with a number of parameters n > 2.

The goodness of fit highlights that the rubbers present the deviation from the ideal entropic behavior, which takes into account the role of entanglements predicted in Marrucci tube rubber theory by the amplification factor A in equations (8) and (9). The goodness of the fitting for blends L8/M20 and L12/M20 confirms the formation of an effective network by the Entanglement locking mechanism.

The badness of fit for the pure rubber M10 would be due to the presence of network defects corresponding to the high concentration of dangling chains.

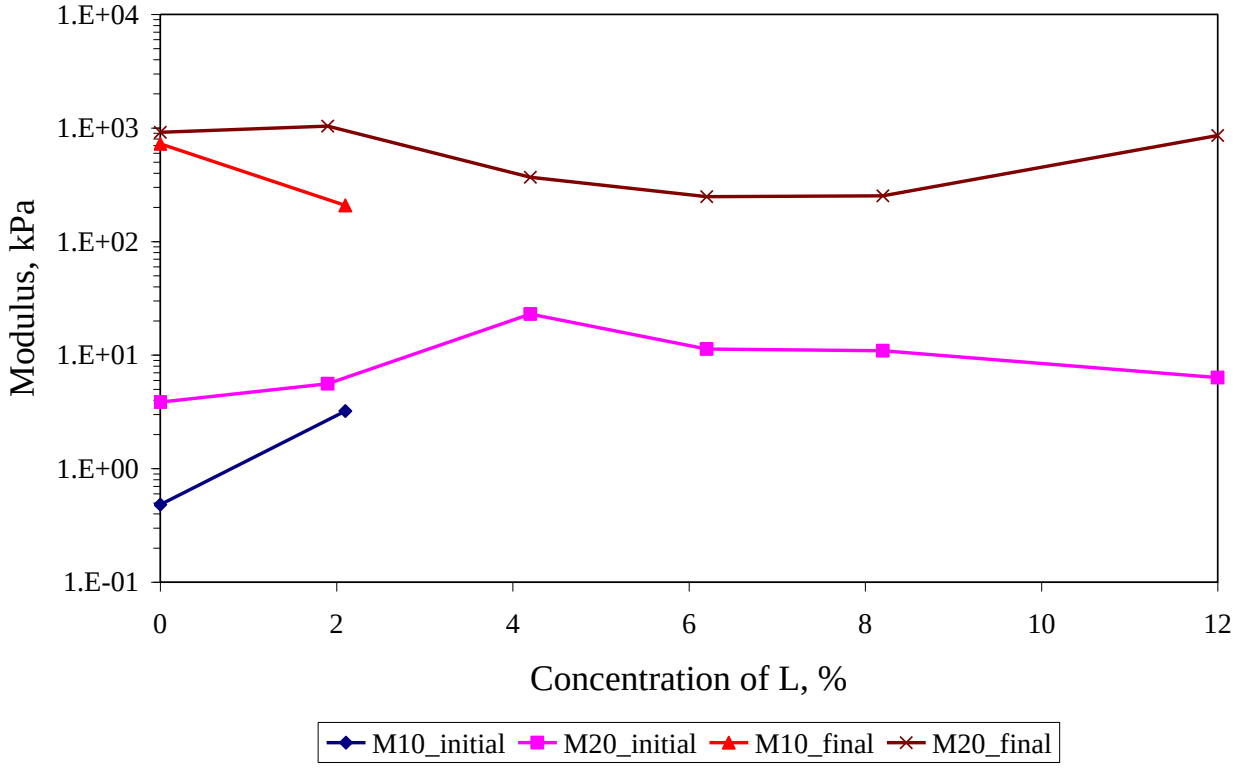

Figure 6. Elastic moduli for rubber blends of Fig. 3. The values at the origin (lower curves) and of 6.75% (upper) are reported. The concentration of the blending agent is reported on the abscissa.

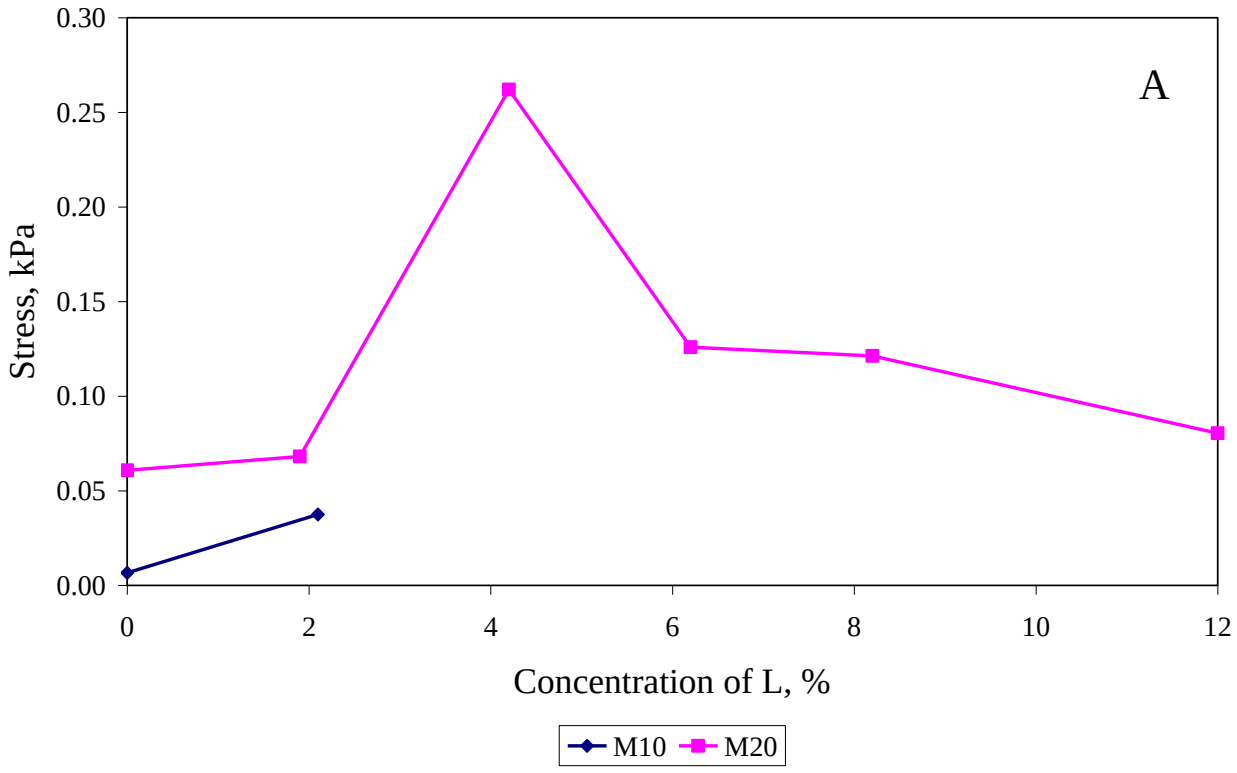

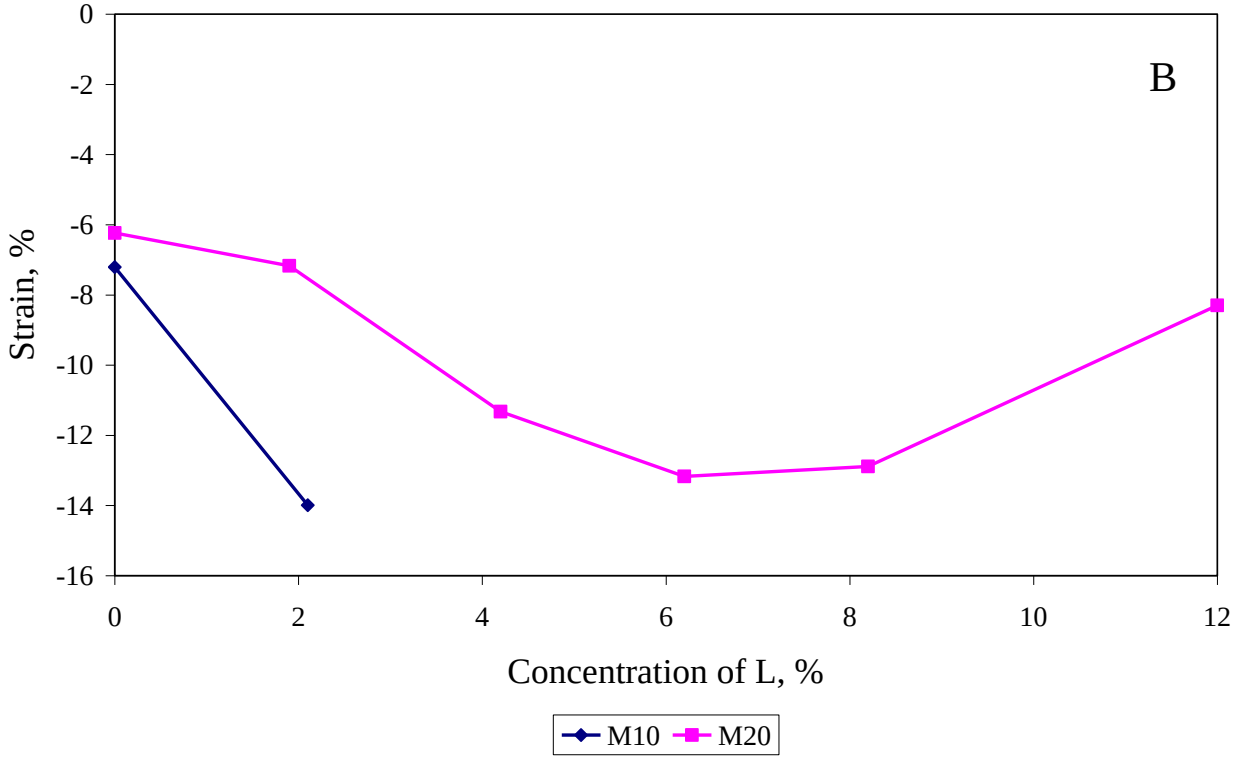

Figure 7. From Fig. 3 the plots of stress at low strain ε = 0.75% (A) and strain at high stress σ = $3.6 \cdot 10^{-2}$ MPa (B) are constructed, as a function of the blending concentration. The concentration of the blending agent is reported on the abscissa.

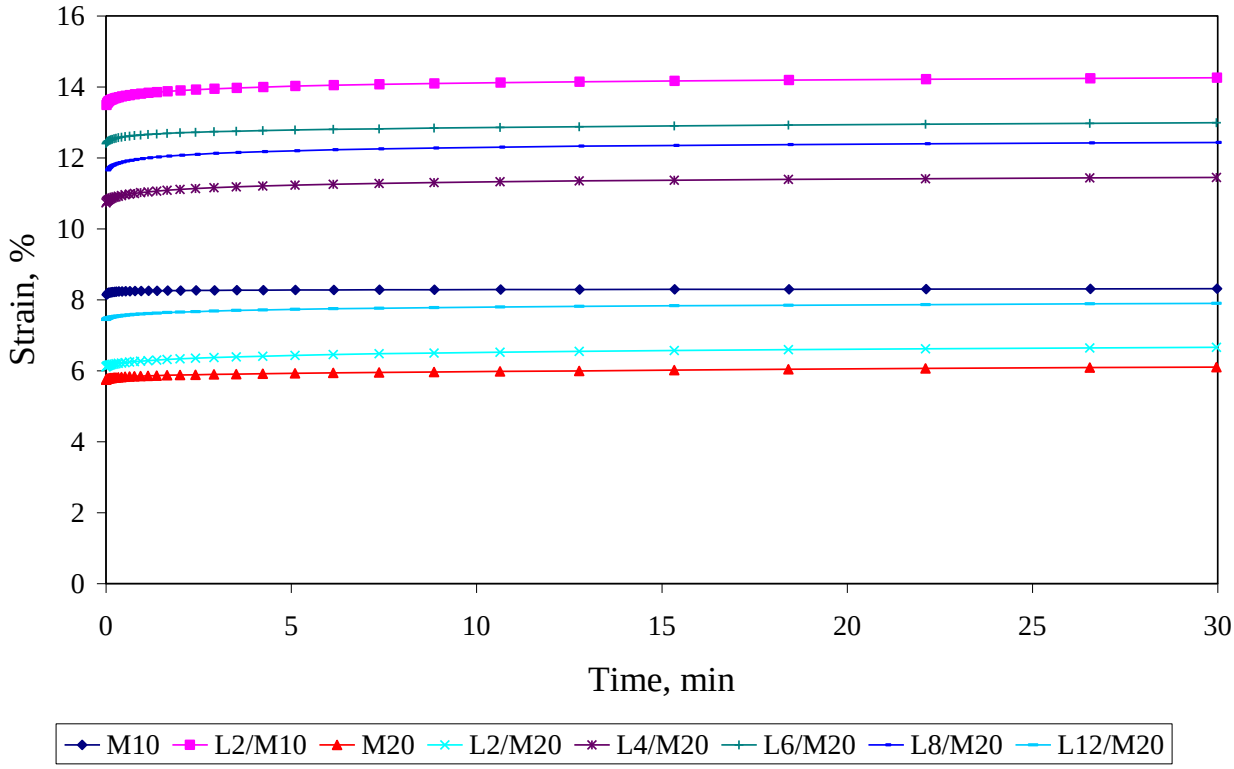

Figure 8. Creep experiments for Low/Medium rubber blends varying the concentration of the Low component and of the curing agent. The constant stress of 30 kPa has been applied.

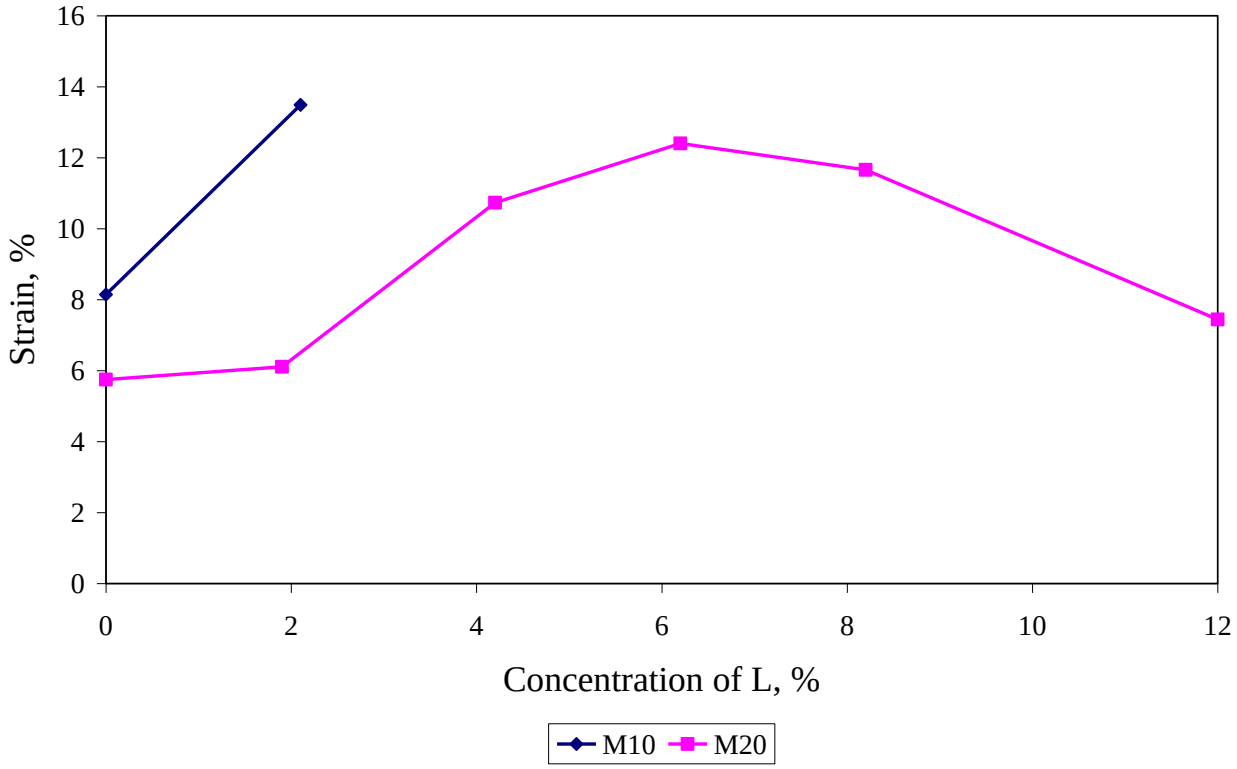

Figure 9. The ultimate strain values of creep deformation for the rubber blends from experiments of Fig. 8. The concentration of the blending agent is reported on the abscissa.

In the creep tests of **Fig. 8**, the constant stress of 30 kPa, corresponding to a high strain in the stress-strain curves, is applied. The compliance experiments and the compliance values reported in **Fig. 9** confirm the trend described by the stress-strain curves of Fig. 3. In fact, for the 20% curing agent L/M blend, the maximum softness (minimum stiffening) is achieved at the 6% composition of the low molecular weight LE-(L) component. Furthermore, blends at concentrations of 8 and 12% show growing stiffening. A similar amplified result is observed for the 10% blend of curing agent for low blending concentrations, as the density and functionality of crosslinks increase.

Therefore, the creep behavior confirms the locking mechanism to the wide deformations previously proposed.

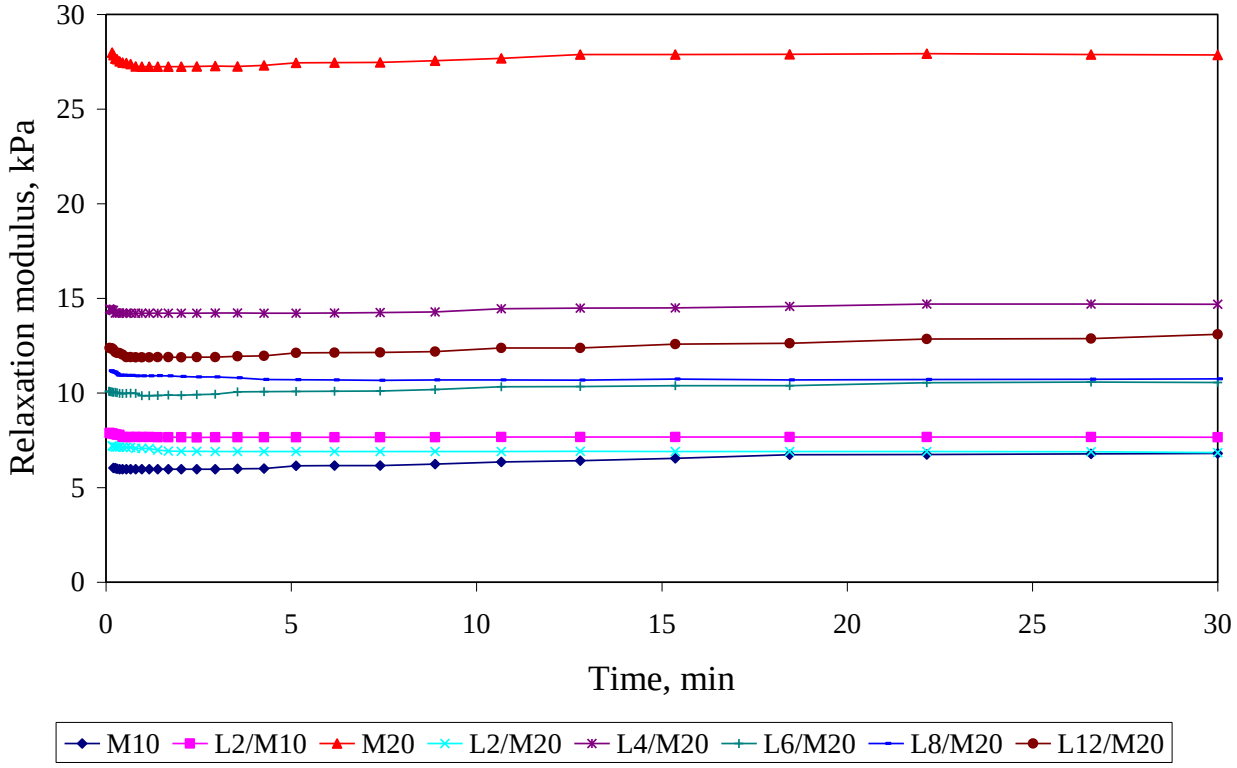

Figure 10. Stress-relaxation experiments for Low/Medium rubber blends varying the concentration of the Low component and of the curing agent. A constant deformation of 1% has been applied.

In the stress-relaxation experiments of **Fig. 10**, an instantaneous and constant deformation of 1% is applied, corresponding to a low deformation in the stress-strain curves of Fig. 6. The trend of E_0 reported in **Fig. 11** does not correspond to the elastic modulus E obtained from the stress-strain curves at the origin, but rather corresponds to a strain of about 3%. The differences are due to the instantaneous deformation imposed in the step-strain experiment and to the slow (delayed) deformation in the stress-strain experiment. The trend of the values of E_0, being fundamental for all the viscoelastic properties of the polymeric materials, must be placed at the base of the proposed interpretative model.

The reference medium component of 20% of curing agent has the highest value of E_0 observed; however, the 4% concentration blend of low component has a relative maximum comparable to the absolute maximum obtained from the stress-strain curves in Figs. 6 and 7. For greater values, from 6 to 12%, an almost constant behavior is observed with a slight increasing trend. On the contrary, as regards the blend of 10% crosslinking and 1.8% of the low component, we observe an increase of E_0 compared to the reference medium component, which confirms the trend of the corresponding stress-strain curve. Substantially, for the 20% crosslinking blend, we observe lower values than the reference component and the maximum at 4% previously described.

The interpretative model of the increase in active chain density and functionality at low deformations takes into account the observed trend.

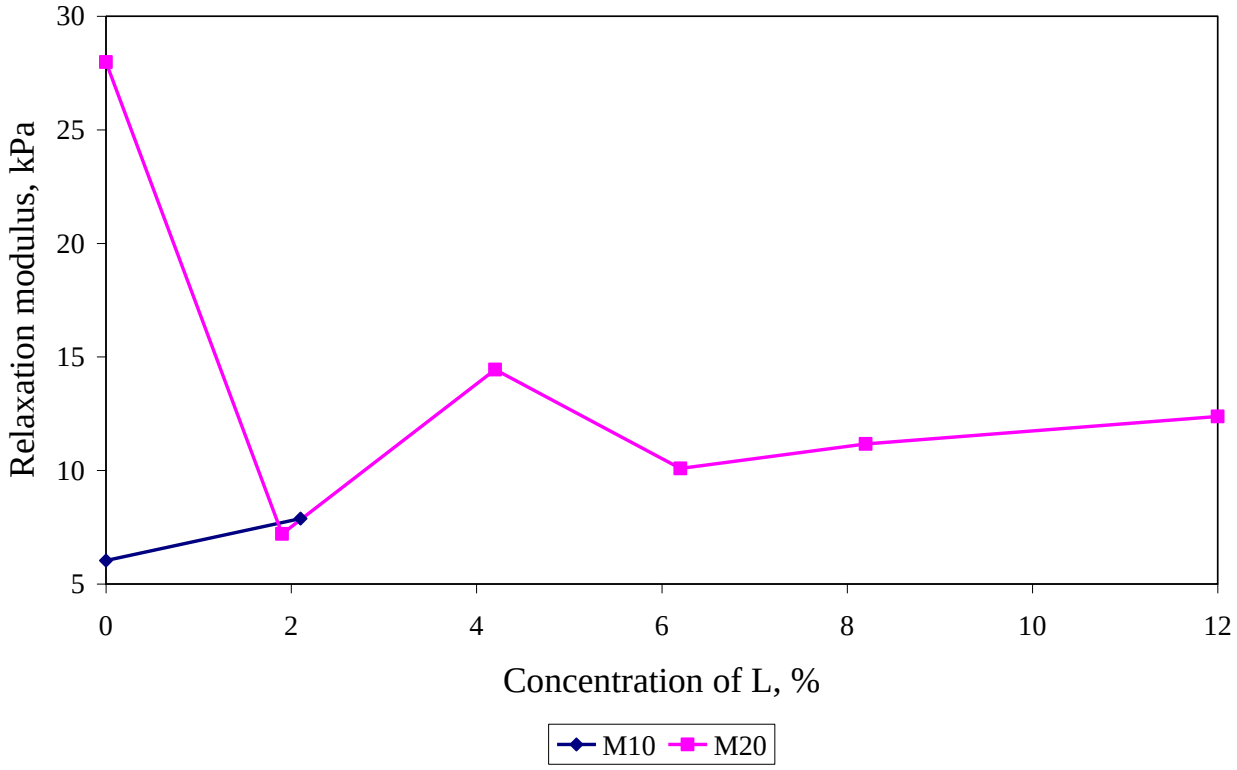

Figure 11. The instantaneous modulus E_0 from stress-relaxation experiment reported in Fig. 10.

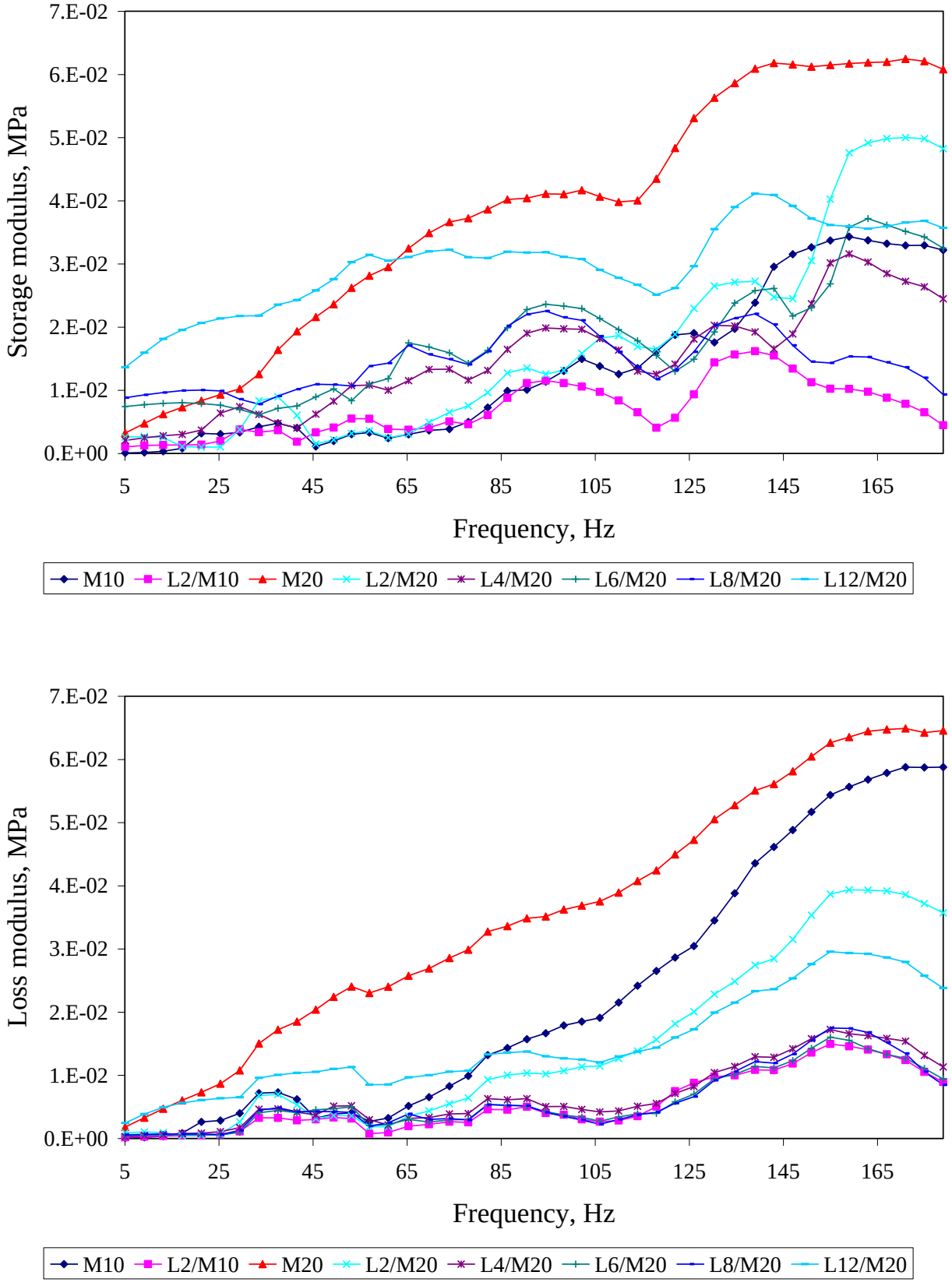

Figure 12. Dynamic-mechanical strain spectra of storage modulus *E'* and loss modulus *E''* for the pure rubbers and blends varying the concentration of curing agent or blending component. The amplitude of 0.05% is applied. Two runs are carried out in order to verify the experimental

reproducibility. The linear frequency spectrum used is helpful in the discussion of the entropic mechanism (see text). A three-point moving average has been applied to spectral curves.

In **Fig. 12** the storage modulus *E′* and the loss modulus *E″* are reported in the whole instrumental frequency range from 1 to 200 Hz for the blends with different contents of the short-chain blending component. The reference rubbers with different contents of curing agent are also reported.

In the high-frequency field, fast relaxations of active chains are observed[37]; in the field of low frequencies the slow relaxation of the dangling chains[11,38] and of the locked chains, according to the proposed model.

The storage modulus *E′* of the 20% crosslinking rubber predominates in the high frequency field, confirming the prevalent contribution of the rigid active chains in the elasticity of the network. As the frequency decreases, inversion points are observed between the considered samples, interpreted as relaxations of the dangling chains. In fact, for frequencies lower than 60 Hz, the storage modulus at blending less than 6% tends towards zero. Conversely, for frequencies lower than 30 Hz the contribution of *E′* of the blends greater than 6% remains significant. These relaxations at higher concentrations of blending would be associated with the reduced mobility of locked entanglements stabilized by the adsorption of free short chains on the overlapped dangling chains (Scheme I). In this way the locked entanglements participate in the elasticity of the rubber network as effective-crosslinks, in agreement with the observed elasticity of the stress-strain curves and the compliance at high deformations and highest concentrations of blending component.

This trend would highlight the low concentration of dangling chains in the reference rubber (ideal rubber) and in the blends at the lowest concentration of the short-chain component.

In the high-frequency field, the high *E′* values of the blends at 12, 6 and 4% confirm the models of the maximum functionalization of the crosslinker (for low concentrations of blending agents) and of the effective-crosslinks in which the short chains give rise to locked dangling chains (at the highest concentration of blending).

The performance of the dissipative module *E″* in Fig. 12b shows the high values associated with the active chains of the pure or slightly modified rubbers at 2% and of the dangling locked chains of the blend at 12%. Significant differences in the values of *E′* in the blends at intermediate composition are not observed.

In the picture of **Scheme II**, a dynamical locking entanglement mechanism is proposed. The vibrational modes of nanosized coil of the short chain among the blobs of entangled chains would give rise to a chaotic dynamics of indefinite period: the fluctuations of interacting particles cannot be in-phase and give the geometrical frustration effect[39]. In the past, one of us (Villani) has proposed a mechanism for the entropic elasticity of elastin (the structural protein responsible for the

elasticity of vertebrate tissues) based on chaotic molecular dynamics of the secondary structure[40,41]. In the present work, the chaotic dynamics of interacting random coils of locked entanglements matches the broad linear spectra of *E'* and *E"* observed at lowest frequency (Fig. 12). According to the Marrucci elasticity theory and Mooney-Rivlin correction, equations (8) and (9), the tube of network chain deforms affinely, in which at the longitudinal stretching factor λ the transversal factors $1/\sqrt{\lambda}$ correspond. Then, the gyration radii of tube blobs between the entanglements, corresponding to the cross section radii, change affinely becoming isomorphic to the random coil of free short chains, until they give rise to the entanglement locking by means of the entropic frustration mechanism proposed. The onset of the entanglement locking should correspond to the trend inversion in the stress-strain curves of Fig. 3 at ε = -1.0 for the L8/M20 and ε = -3.5% for L12/M20 blends.

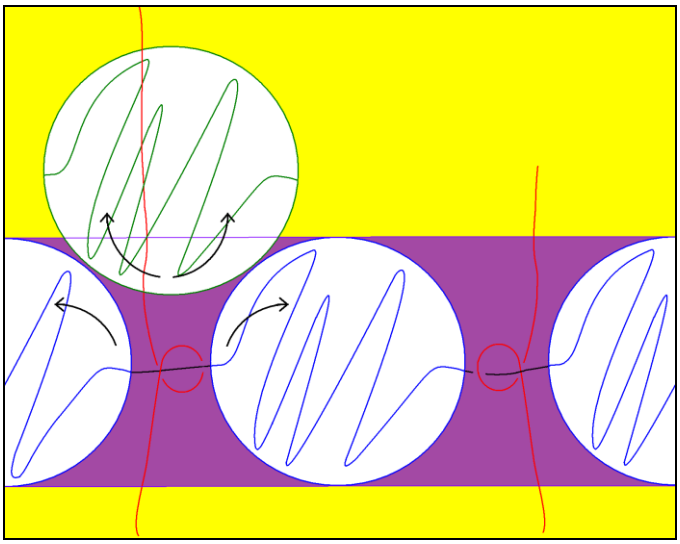

Scheme II. The dynamical locking entanglement picture: the random-coil of short chain is adsorbed on entanglement site of dangling chains (see Scheme I) and by means of many-body interactions it gives a high entropy dynamics. The arrows indicate the frustration effect among three isodimensional coils rotating in incompatible way.

Conclusions

In our previous work we have shown that a homologous PDMS liquid blend consisting of unentangled short chains in long entangled ones presents an anomalous enhancement in rheological properties: increase in viscosity η_0, relaxation modulus E_0, dynamic moduli *E'* and *E"* and decrease in compliance $J(t)$. The rheological increase was interpreted by means of locking mechanism in which entanglements are constrained by the absorption of short chains: a target was to verify if the

entanglement locking mechanism played also a role in the homologous rubber blends of short chains in long chains.

The stress-strain curves, the creep and step-strain, and dynamic-mechanical experiments showed a complex behavior of the PDMS rubber blend formulations. The key findings from this study are as follows:

(a) The pure rubber networks of reference are made by a set of predominantly active chains, which takes into account both the density of the crosslinks and their functionality.

(b) In the mechanical experiments, the behavior at small strain can be interpreted on the basis of the classical rubber theory taking into account the increase of the density of the active chains as a function of the concentration of the short chain blending agent. The set of stress-strain curves with different composition of the blending agent shows a behavior depending on the degree of deformation. In particular, for $\varepsilon < 0.01$ the 4% sample in blending component has the maximum elastic modulus; for $0.01 < \varepsilon < 0.04$ is the pure component to be the most elastic; the elasticity decreases with the increase of the minor component and is reversed starting from a 6% composition.

(c) At low concentration of blending agent, the most likely event is the formation of short active chains, which leads to an increase in the density of active chains. This will result in a corresponding increase in the elastic modulus (in the field of small deformations) according to the theories of the ideal rubber elasticity.

(d) As the blending agent concentration increases, the formation of dangling chains increases to the detriment of the concentration of active chains, giving the decrease of the elastic modulus.

(e) At a sufficiently high concentration of blending agent, the crosslinkers will be saturated by long and short dangling chains. This will correspond to a minimum in the elastic properties of the blend.

(f) At higher concentrations of blending agent, we have the adsorption of short chains on entanglement sites involving long dangling ends. In this way, the entanglement locking gives rise to the formation of effective crosslinks involving the dangling-active chains or long-long dangling ones. The phenomenon of entanglement locking corresponds to high entropy dynamics of chains, the increase of active chain density and crosslink functionality with the improvement of elastic modulus of the rubber, according to Marrucci tube network theory and Mooney-Rivlin correction.

(g) At large strain, the pure component turns out to be the most rigid (high modulus E, E_0 and low compliance to equilibrium J_e^0) followed by the 12% one and therefore by those with a lower concentration of blending agent. The increase in elasticity at low blending concentrations and high deformation cannot be interpreted in terms of trapped entanglements, in fact the density of these defects should decrease as the concentration of active short chains increases, therefore the role could be played by the proposed Entanglement Locking model.

(h) The entanglement locking involving dangling chains and active chains enhances the relaxation times and increases the effective crosslink density, justifying the maximum elasticity for the blend to 12%. The proposed mechanism of locked entanglement would be consistent with the maximum of the viscoelasticity at small strain and low concentration of the minor component, and with the maximum elasticity at large strain and high concentration of the blending agent. The broad spectra of *E'* and *E''* at the lowest frequencies of the dynamic-mechanical experiments would be due to the high entropy chaotic dynamics of entanglement locking.

The role of Entanglement Locking in the unique viscoelasticity at high deformation is a possible advancement of rubber elasticity theory, and opens to both modelling and application developments of polydimethylsiloxane elastomers.

Acknowledgments

We wish to thank anonymous referees for the very useful suggestions.

References

[1] S. Moghadam, I. S. Dalal, R. G. Larson, Slip-Spring and Kink Dynamics Models for Fast Extensional Flow of Entangled Polymeric Fluids, *Polymers* **2019**, *11*, 465.

[2] A. E. Likhtman, Single-Chain Slip-Link Model of Entangled Polymers: Simultaneous Description of Neutron Spin-Echo, Rheology, and Diffusion, *Macromolecules* **2005**, *38*, 6128–6139.

[3] M. H. Nafar Sefiddashti, B. J. Edwards, B. Khomami, Individual chain dynamics of a polyethylene melt undergoing steady shear flow, *Journal of Rheology* **2015**, *59*, 119–153.

[4] P.-G. de Gennes, *Scaling Concepts in Polymer Physics*, Cornell University Press, Ithaca **1979**.

[5] M. Doi, S. F. Edwards, *The Theory of Polymer Dynamics*, Oxford University Press, NY **1988**.

[6] J. Duhamel, A. Yekta, M. A. Winnik, T. C. Jao, M. K. Mishra, I. D. Rubin, A blob model to study polymer chain dynamics in solution, *J. Phys. Chem.* **1993**, *97*, 13708–13712.

[7] G. Marrucci, Relaxation by reptation and tube enlargement: A model for polydisperse polymers, *J. Polym. Sci. Polym Phys. Ed.* **1985**, *23*, 159–177.

[8] M. J. Struglinski, W. W. Graessley, Effect of polydispersity on the linear viscoelastic properties of entangled polymers. 1. Experimental observation for binary mixtures of linear polybutadiene, *Macromolecules* **1985**, *18*, 2630–2643.

[9] V. Villani, V. Lavallata, Unusual Rheological Properties of Lightly Crosslinked Polydimethylsloxane, *Macromol. Chem. Phys.* **2017**, *218*, 1700037.

[10] V. Villani, V. Lavallata, Unexpected Rheology of Polydimethylsiloxane Liquid Blends, *Macromol. Chem. Phys.* **2018**, *219*, 1700623.

[11] A Batchelor, G.K., The effect of Brownian motion on the bulk stress in a suspension of spherical particles. Journal of Fluid Mechanics, 1977. 83(01): p. 97-117.

[12] H. M. James, E. Guth, Theory of the Elastic Properties of Rubber, *J. Chem. Phys.* **1943**, *11*, 455–481.

[13] H. M. James, E. Guth, Simple presentation of network theory of rubber, with a discussion of other theories, *J. Polymer Sci.* **1949**, *4*, 153–182.

[14] P. J. Flory, J. Rehner, Statistical mechanics of cross-linked polymer networks: I, rubberlike elasticity. *J. Chem. Phys.* **1943**, *11*, 512–520.

[15] P. J. Flory, J. Rehner, Statistical mechanics of cross-linked polymer networks: II, swelling. *J Chem. Phys.* **1943**, *11*, 521–526.

[16] G. Ronca, G. Allegra, An approach to rubber elasticity with internal constraints, *J. Chem. Phys.* **1975**, *63*, 4990–4997.

[17] P. J. Flory, Statistical thermodynamics of random networks, *Proc. R. Soc. Lond. A* **1976**, *351*, 351–380.

[18] S. F. Edwards, Theory of rubber elasticity, *Br. Polym. J.* **1977**, *9*, 140–143.

[19] G. Marrucci, *Rubber Elasticity Theory. A Network of Entangled Chains*, *Macromolecules* **1981**, *14*, 434-442.

[20] J. E. Mark, Elastomers with multimodal distributions of network chain lengths, *Macromolecular Symposia* **2003**, *191*, 121-130.

[21] F. Campise, D. C. Agudelo, R. H. Acosta, M. A. Villar, E. M. Vallés, G. A. Monti, D. A. Vega, Contribution of Entanglements to Polymer Network Elasticity, *Macromolecules* **2017**, *50*, 2964−2972.

[22] S. H. Yoo, L. Yee, C. Cohen, Effect of network structure on the stress–strain behaviour of endlinked PDMS elastomers, *Polymer* **2010**, *51*, 1608–1613.

[23] S. H. Yoo, C. Cohen, C.-Y. Hui, Mechanical and swelling properties of PDMS interpenetrating polymer networks, *Polymer* **2006**, *47*, 6226–6235.

[24] H. F. Mark (Editor), Silicones in *Encyclopedia of Polymer Science and Technology*, Wiley, NY **2014**.

[25] G. D. Genesky, B. M. Aguilera-Mercado, D. M. Bhawe, F. A. Escobedo, C. Cohen, Experiments and Simulations: Enhanced Mechanical Properties of End-Linked Bimodal Elastomers, *Macromolecules* **2008**, *41*, 8231-8241.

[26] I. D. Johnston, D. K. McCluskey, C. K. L. Tan, M. C. Tracey, Mechanical characterization of bulk Sylgard 184 for microfluidics and microengineering, *J. Micromech. Microeng.* **2014**, *24*, 035017.

[27] K. Urayama. T. Kawamura, S. Kohjiya, Structure-mechanical property correlations of model siloxane elastomers with controlled network topology, *Polymer* **2009**, *50*, 347–356.

[28] C. M. Roland, *Viscoelastic Behavior of Rubbery Materials*, Oxford University Press, NY **2011**.

[29] J. M. Chalmers, R. J. Meier, *Molecular Characterization and Analysis of Polymers*, Elsevier, Amsterdam **2008**.

[30] P. J. Flory, *Principles of Polymer Chemistry*, Cornell University Press, **1953**.

[31] V. Villani, *Introduzione alla Scienza dei materiali polimerici*, Aracne editrice, Roma **2017**.

[32] E. Delebecq, F. Ganachaud, Looking over Liquid Silicone Rubbers: (1) Network Topology vs Chemical Formulations, *ACS Appl. Mater. Interfaces* **2012**, *4*, 3340–3352.

[33] N. Kumar, V. V. Rao, Hyperelastic Mooney-Rivlin Model: Determination and Physical Interpretation of Material Constants, *MIT International Journal of Mechanical Engineering* **2016**, *6*, 43-46.

[34] L. H. Sperling, *Introduction to Physical Polymer Science*, 4th Edition, Wiley, Hoboken **2006**.

[35] M. Rubinstein, Elasticity of Polymer Networks, *Macromolecules* **2002**, *35*, 6670–6686.

[36] *Ullmann's Polymers and Plastics, Volume 2*, Wiley-VCH, Weinheim **2016**.

[37] H. Takahashi, Y. Ishimuro, H. Watanabe, Viscoelastic Behavior of Scarcely Crosslinked Poly(dimethyl siloxane) Gel, *Journal of the Society of Rheology, Japan* **2006**, *34*, 135-145.

[38] X. Wang, J. Mi, J. Wang, H. Zhou, X. Wang, Multiple actions of poly(ethylene octene) grafted with glycidyl methacrylate on the performance of poly(lactic acid), *RSC Adv.* **2018**, *8*, 34418.

[39] R. Moessner, A. Ramirez, Geometrical frustration, *Physics Today* **2006**, *59*, 24-29.

[40] V. Villani, L. D'Alessio, A. M. Tamburro, Conformational non-linear dynamical behavior of the peptide Boc-Gly-Leu-Gly-Gly-NMe, *Journal of the Chemical Society. Perkin Transactions 2* **1997**, *11*, 2375–2385.

[41] V. Villani, A. M. Tamburro, J. M. Zaldivar Comenges, Conformational chaos and biomolecular instability in aqueous solution, *Journal of the Chemical Society. Perkin Transactions 2* **2000**, *11*, 2177–2184.